DOI: 10.5327/Z2317-4889201400020003

ARTICLE

Dating low-grade metamorphism and deformation of the Espinhaço Supergroup in the Chapada Diamantina (Bahia, NE Brazil): a K/Ar fine-fraction study

Datando os baixos graus de deformação e metamorfismo do supergrupo Espinhaço na Chapada Diamantina (Bahia, NE Brasil): um caso de estudo K-Ar em frações finas

Annette Süssenberger[1]*, Benjamim Bley de Brito Neves[2], Klaus Wemmer[3]

ABSTRACT: This study focuses on the northernmost part of the Mesoproterozoic Espinhaço Supergroup that crops out in the Chapada Diamantina. The fine-fraction K/Ar dating obtained on slightly metamorphosed sediments of the siliciclastic Espinhaço Supergroup shows a polyphase deformation history that corresponds to the Brasiliano (Pan-African) orogenic cycle. The isotopic results are interpreted to indicate three age domains coincident with three structurally different domains. Constrained by the Kübler Index ('illite crystallinity') and illite polytypism, the thermal conditions generated during the tectonic activity show a gradual trend from the craton margins to the interior from epizonal to diagenetic. The northern Chapada Diamantina is situated in the foreland of the Riacho do Pontal belt and comprises the sediments of the Espinhaço Supergroup northeast of the Irecê basin. The K/Ar ages for < 2 µm illite fractions range between 645 and 621 Ma [mean 637±9 Ma (2σ)] and for < 0.2 µm fraction range between 625 and 603 Ma [mean 614±9 Ma (2σ)]. Samples from the central Chapada Diamantina east of the Irecê basin are not affected by a Brasiliano deformation event and therefore, the N-S-trending structures are assumed to be older. The deformation of the southern Chapada Diamantina was established in conjunction with the formation of the Araçuai orogenesis and the inversion and reactivation of the Paramirim impactogen. The last stage of deformation in this area is recorded by the K/Ar fine-fraction dating between 470 and 460 Ma.

KEYWORDS: Chapada Diamantina; Espinhaço Supergroup; K/Ar fine-fraction dating; illite.

RESUMO: *Este trabalho focaliza a parte mais setentrional do Supergrupo Espinhaço que aflora na Chapada Diamantina-Bahia. Frações finas K-Ar conduzidas em metassedimentos siliciclásticos de baixíssimo grau metamórfico mostraram uma história polifásica de deformação que corresponde ao Ciclo Brasiliano (=Pan Africano). Os resultados interpretados de dados isotópicos estão indicando três domínios de idade, os quais coincidem com três distintos domínios estruturais. De acordo com o índice Kübler (cristalinidade da illita) e o politismo da illita, as condições geradas durante a atividade tectônica mostram uma gradual mudança das margens do cráton para o seu interior, de condições epizonais para condições nitidamente diagenéticas. A porção norte da Chapada Diamantina está situada no antepaís do sistema de dobramentos Riacho do Pontal e isto compreende os sedimentos do Supergrupo Espinhaço a nordeste da chamada Bacia de Irecê. As idades K-Ar para frações < 2µm de ilita variam de 645 e 621 Ma (Média de 637±9 Ma, [2σ]) e para frações < 2µm as idades variam entre 625 e 603 Ma (média 614±9 Ma, [2σ]). Amostras da parte central da Chapada a leste da Bacia de Irecê não foram afetados pelo evento de deformação do brasiliano, e por conseguinte o trend estrutural dominante N-S é considerado mais antigo. A deformação da parte sul da chapada Diamantina foi estabelecida em conjunção com o desenvolvimento da orogênese Araçuaí e a inversão e reativação do impactógeno de Paramirm. O último estágio de deformação nesta área é registrado por frações finas de K-Ar no âmbito de 470-460 Ma*

PALAVRAS-CHAVE: *Chapada Diamantina; Super-grupo Espinhaço; frações finas K-Ar; Illita*

[1]University of Geneva, Switzerland. *E-mail: annette.suessenberger@unige.ch*

[2]Institute for Geoscience, Universidade de São Paulo - USP, São Paulo (SP), Brasil. *E-mail: bbleybn@usp.br*

[3]Geoscience Center, University of Göttingen, Göttingen, Germany. *E-mail: kwemmer@gwdg.de*

*Corresponding author

Manuscrito ID 30062. **Recebido em:** 14/05/2014. **Aprovado em:** 09/06/2014.

INTRODUCTION

The study area Chapada Diamantina (Bahia, NE Brazil) represents the northern part of the wide Espinhaço basin (extending from Minas Gerais to Piaui, along the São Francisco Craton, > 1,100 km) (Fig. 1). In this study the focus will be on the northernmost part of the mesoproterozoic Espinhaço Supergroup, which crops out in the Chapada Diamantina. Here, the sediment succession mainly consists of quartzites and metapelites and is unconformably overlying the basement rocks of the São Francisco Craton (Pedreira & De Waele 2008 and references therein). After an early stage of rifting, the Espinhaço Supergroup underwent metamorphism and deformation during the amalgamation of the western Gondwana paleocontinent during the so-called neoproterozoic Brasiliano-orogenic cycle between 650 and 550 Ma (Schobbenhaus 1996; Danderfer 2000). This collision was responsible for the present structural configuration of the mesoproterozoic sediment sequence, including a km-scale folding with dominating NNW, in parts SW-trending axes (Alkmim *et al*. 2006). Alvarenga and Dardenne (1978) showed that extensively aligned faults, mostly NNE-SSW, may represent basement structures reactivated during sedimentation.

Because fairly little is currently known about Mesoproterozoic events within the São Francisco Craton, mainly because of lack of reliable age determination, it is not surprising that a possible folding of the Espinhaço Supergroup before the Neoproterozoic Brasiliano orogeny is controversial (Fuck *et al*. 2008; Cordani *et al*. 2010). However, the foreland fold and thrust belt recorded in the Irecê basin, in the northwestern part of the Chapada Diamantina, is characterized by E-W structures and is unconformably overlying the NNW-SSE folding observed in the Espinhaço strata. The structural polarity of the latter is due to the active margin of the São Francisco Craton, and can be attributed to the amalgamation of Gondwana at about 600 – 550 Ma (Cordani *et al*. 2010).

Previous efforts to date the deformation were made on adjacent units but not for the Espinhaço Supergroup (in the Chapada Diamantina) itself. Cordani *et al*. (1992) reported K/Ar cooling ages in minerals separated from the granite–orthogneiss complex Lagoa Real (southwest of the Chapada Diamantina), which fall within the interval of 570 – 500 Ma, indicating the influence of a late Brasiliano tectonothermal cycle. Investigations on undeformed carbonates of the Una Group were carried out by Misi and Veizer (1998), suggesting that the sedimentation (670 – 600 Ma) of the Saltire Formation (Una Group, Irecê Basin) and of the correlative units of the Bambuí Group (São Francisco Basin) was coeval with the onset of the Brasiliano tectonic cycle.

The present study aims to elucidate the deformation history of the Chapada Diamantina and its supposed relation to an orogenic cycle, either Pan-African/Brasiliano or Grenvillian. Besides structural and tectonic analyses, the K/Ar fine-fraction dating is an important tool for reconstruction of the deformation history of very low grade metamorphic rocks. This method has proved to be a very useful technique dating illites formed by prograde metamorphic reactions during the deformation (Ahrendt *et al*. 1978; Clauer *et al*. 1995, 1997). In particular, metapelitic rocks proved to be very suitable because of their rheological properties that make them highly sensitive even to minor variations in the regional stress field. The cleavage planes on which the newly crystallized illites are expected are in this context of particular importance and will be used in an attempt to shed some light on the final low-grade deformation events.

The age of synkinematically newly grown illites was determined using K/Ar geochronology on fine mineral fractions. This isotopic method was combined with measurements of the illite crystallinity (expressed as Kübler Index) and polytype quantification to unravel the degree of metamorphism and a possibly polyphase thermal overprinting in the Chapada Diamantina. The presented results are considered within the frame of the regional tectonic acting on the southwestern margin of Gondwana.

GEOLOGICAL SETTING

The sediments of the Chapada Diamantina comprise the northwestern part of the São Francisco Craton and are the focal point of this study. The eastern part of the São Francisco Craton underwent rifting during Mesoproterozoic times, leading to the development of the wide Espinhaço basin and the Paramirim valley. What at first began as failed rift resulted in the formation of sag basins that were filled with sandstones, conglomerates, fine-grained rocks and limestones, summarized as Espinhaço Supergroup (Pedreira & De Waele 2008 and references therein). The onset of sedimentation, determined by U-Pb analyses of detrital zircons, yielded ages between 1.8 and 1.76 Ga (Turpin *et al*. 1988; Machado *et al*. 1989; Cordani *et al*. 1992; Babinski 1993). This approximately 2-km-thick sediment succession crops out in three domains namely Chapada Diamantina, Northern- and Southern Espinhaço in which all are related to the orographic system Espinhaço Range. In the Chapada Diamantina, the Espinhaço Supergroup has been divided into three groups that comprise six formations; from base to top, Rio dos Remédios (Ouricuri do Ouro Fm.), Paraguaçu (Mangabeira Fm., Guiné Fm.) and Chapada Diamantina

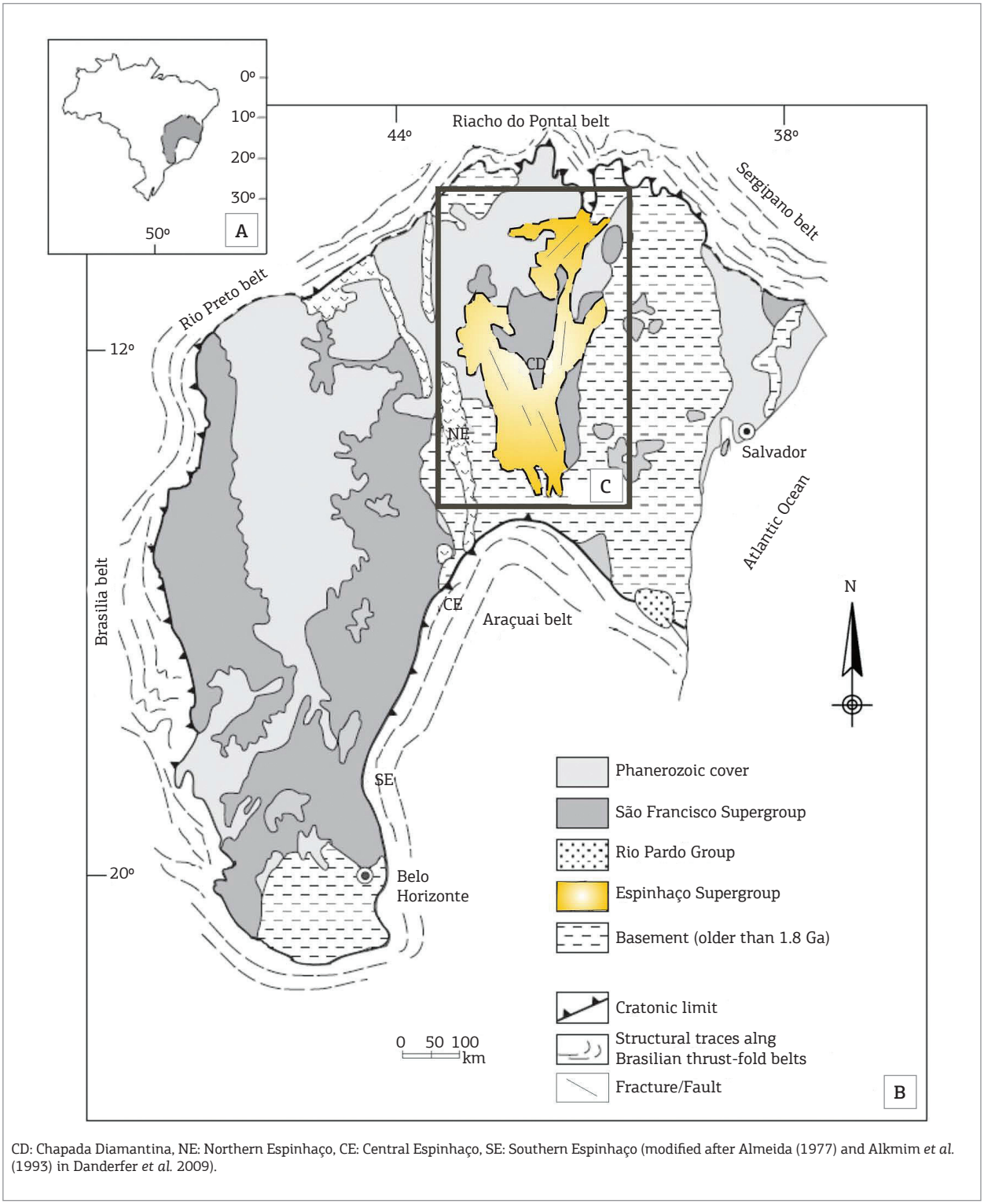

CD: Chapada Diamantina, NE: Northern Espinhaço, CE: Central Espinhaço, SE: Southern Espinhaço (modified after Almeida (1977) and Alkmim *et al.* (1993) in Danderfer *et al.* 2009).

Figure 1. (A) Map of Brazil with highlighted São Francisco Craton. (B) Geological map of the São Francisco Craton and surrounding belts. (C) The working area is marked by the black rectangular.

group (Tombador Fm., Caboclo Fm and Morro do Chapéu Fm.) (Inda & Barbosa 1978; Pedreia 1994; Pedreia & Rocha 2004).

The Chapada Diamantina domain, situated in the central part of the Bahia state, is limited to the north and south by Brasiliano orogenic belts that circumscribe the foreland

of the São Francisco Craton: the Riacho do Pontal belt and Araçuai belt. The western perimeter is formed by the Paramirim River and the eastern border by the Jacobina range.

Structural lineaments

The structural lineaments (folds) that cross the Mesoproterozoic sediment cover of the Chapada Diamantina are evidence enough to show that the sediments were affected by different deformation events that are linked to the surrounding fold and thrust belts. The NNW-SSE-trending Paramirim impactogen divides the São Francisco Craton in two geological domains: on the western side the Meso- and Neoproterozoic sediments of the Espinhaço Supergroup and Bambuí Group, and on the eastern side the equivalent sediment sequences of the Chapada Diamantina and Una Group. The Chapada Diamantina can structurally be divided in at least three sections, which show as a far field response to the intense deformation that took place along the craton margin, NNW-SSE-trending fold axes as in the southwest, NNE-SSW-trending fold axes as in the central part, or WSW-ENE-trending fold axes to the north. Those folded and re-folded structures prove an earlier polyphasic deformation of the Espinhaço Supergroup, which is until now supposedly attributed to a Brasiliano orogeny. According to Torquato and Fogaça (1981) the deformation in the Chapada Diamantina increases progressively from north to south and does not exceed the greenschist facies based on illite crystallinities from the Tombador formation. Whereas, a deformation under greenschist facies conditions is recorded for the Morro do Chapéu formation (Brito Neves *et al*. 2012).

MATERIALS AND METHODS

We collected fresh metapelitic material from 10 sample localities in the Chapada Diamantina, which was subjected to K/Ar and X-ray diffraction (XRD) analyses to define the age of the deformation under lower greenschist facies conditions (Tab. 1, Fig. 2). The samples are covering a N-S section of roughly 200 km.

All samples were cleaned of weathered crusts and subsequently, gently crushed to avoid artificial fragmentation of the original grain components by a shatter mill and passed through a 63-μm sieve. The size fractions (< 2 and 2 – 6 μm) were separated by differential settling in distilled water according to Stoke's law (Atterberg method). Enrichment of the grain size fraction < 0.2 μm was carried out by centrifugation, following the procedure described in Wemmer (1991). The size fractions were collected using a Millipore filter. Subsequently, the concentrates were subjected to isotope measurements and

Table 1. Compilation of sample localities and stratigraphic position

Sample	Coordinates, UTM zone 24S	Description	Stratigraphic Formation
BBB 11-09	0285693/ 8712688	Metapsammite	Caboclo
BBB 13-09	0259148/ 8781026	Metapsammite	Morro do Chapéu
BBB 29-09	0186179/ 8609916	Metapelite	Caboclo
BBB 32-09	0201953/ 8526374	Metapelite	Guiné
BBB 33-09	0201953/ 8526374	Metapelite	Guiné
BBB 34-09	0205766/ 8530302	Phyllite	Ouricuri do Ouro
BBB 38-09	0186649/ 8559826	Metapsammite	Guiné
CHD-R-D3	0231463/ 8877079	Metapelite	Morro do Chapéu
CHD-R-D4	0231463/ 8827099	Metapelite	Morro do Chapéu
CHD-R-C3	0231109/ 8827178	Metapelite	Morro do Chapéu

XRD analyses. The XRD analyses were carried out using a PW 1800 Phillips diffractometer (CuKα radiation, at 45 kV and 40 mA conditions). Oriented clay aggregates were prepared onto glass slides (Moore & Reynolds 1997) and analyzed by XRD both after airdrying and after ethylene glycol treatment. From the resulting XRD patterns, we determined:

- The full-width at half maximum (FWHM), also known as Kübler Index (KI), of the illite 001 peak (Kübler 1967). The illite crystallinity is a function of the grain size and increases with increasing grain size. The determination of the illite crystallinity is performed on glass plates, according to Weber (1972), with "thin" texture

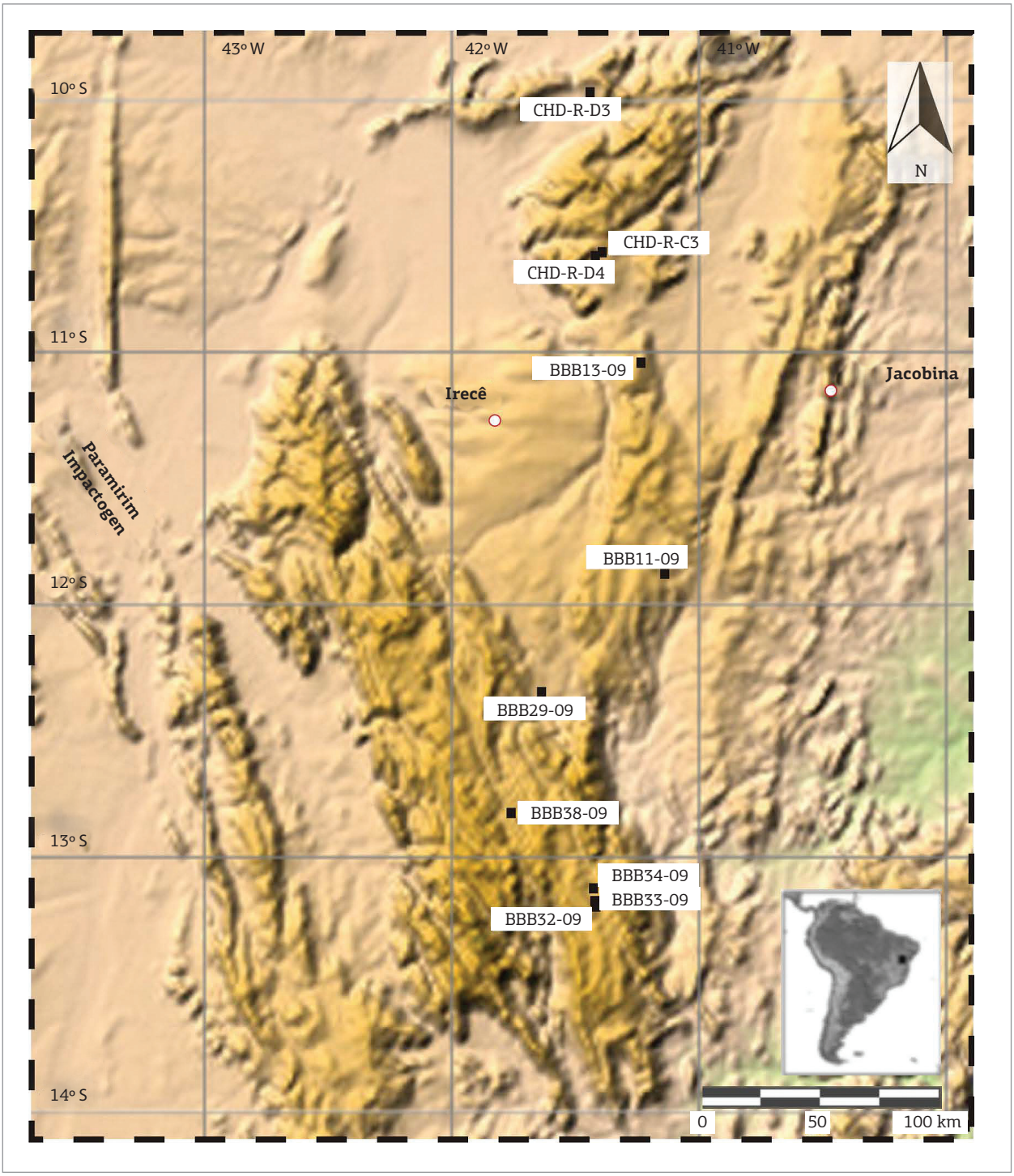

Figure 2. Regional digital elevation model showing the location of the samples analyzed in this study.

compounds prepared using 1.5 – 2.5 mg/cm². Samples were scanned from 7 to 10° 2Θ, using a step size of 0.01° 2Θ and an integration time of 4 s. The illite crystallinity was determined using a computer program (Idefix) developed at the Geosciences Center of the University of Göttingen by Ullemeyer. Limits between the fields of diagenesis, achi-, and epizone are given by 0.420° Δ2Θ CuKα and 0.250° Δ2Θ CuKα, respectively (Kübler 1967; Marheine 1997).

- The mineral content to verify the presence of illite and to rule out the presence of other K-bearing minerals that may influence the age data. To identify the mineral content, we performed a stepscan (0.02° 2Θ) in the range from 4 to 70° 2Θ.
- Polytype quantification. We prepared the size fraction as random powder mounts using the sideload method described and recommended in Moore and Reynolds (1997) and Grathoff *et al.* (1998). The concentration of different polytypes is determined by measuring the area/intensity of polytype-specific peaks (in case of $2M_1$ of five specific peaks) and rationing them against the area/intensity of a peak at 2.58 Å, which is common at both polytypes (Grathoff & Moore 1996). These methods represent a significant improvement compared to earlier techniques that relied on the measurement of only one specific $2M_1$ peak such as from Hower *et al.* (1963), summarized in Grathoff and Moore (1996). Pevear (1992) and Grathoff and Moore (1996) used different polytypes to distinguish diagenetic from detrital illite and suggested methods for extrapolating to the ages of diagenetic and detrital illites in shales. By plotting the K/Ar ages of at least three size fractions of illite against the percentage of illite that is detrital ($2M_1$), extrapolation to zero detrital illite gives the age of diagenesis, and extrapolation to zero authigenic/diagenetic illite gives the age of the detrital illite. It is noteworthy that based on XRD analysis, high-temperature $2M_1$ illite cannot be distinguished from muscovite, which is also a $2M_1$ polytype.

The samples were scanned from 16 to 44° 2Θ in the step-scanning mode with a step size of 0.05° and a counting time of at least 30 s/step to gain a high peak-to-background resolution. We prevented the problem of peak interferences with other clay minerals (kaolinite) by heating the sample to 550°C for 1 h, which caused dehydroxylation of kaolinite.

The age determination analyses proceeded in two stages, an analysis of potassium and an analysis of argon. The potassium (K_2O) was analyzed in duplicates by atomic absorption spectrophotometer using a PerkinElmer 5100 PC. The samples were dissolved in a mixture of HF and HNO_3 followed by addition of CsCl suspension (12.5%) as an internal standard and ionization buffer for alkali metals. The pooled error of the duplicate potassium determinations in samples and standards is more than 2%. For Ar analyses, the samples were pre-heated at high vacuum at 120°C for at least 24 h to reduce the amount of atmospheric argon added to the mineral surfaces during handling. The argon isotopic composition was analyzed in a Pyrex glass extraction and purification line coupled to a VG 1200 C noble-gas mass spectrometer operating at static mode. The amount of radiogenic ^{40}Ar was determined by isotope dilution method using a highly enriched ^{38}Ar spike (Schuhmacher 1975), which was calibrated against the international biotite standard HD-B1 (Fuhrmann *et al.* 1987). The extracted gases were purified in a multistage process by Ti- and SORB-ACs getters. The reproducibility of Ar isotopic results was controlled by repetitive analysis of the standard HD-B1. The obtained values were considered to be satisfying and no corrections were applied to the raw data. The K/Ar ages were calculated with the usual decay constants (Steiger & Jäger 1977), the overall error being < 1% (2σ).

RESULTS

XRD mineralogy

The mineral content of metapelites in the Espinhaço Supergroup is dominated by illite, kaolinite and quartz with minor amounts of hematite, pyrophyllite and gypsum (Tab. 2). However, there is no indication that any other potassium- or calcium-bearing mineral disturbs the isotopic system.

Illite crystallinity index

To identify retrograde grown mixed-layered minerals, we compared the KI values of oriented air-dried and glycolated samples. As the data yield identical values, the existence of smectite-type minerals can be excluded. Differences between both values are not significant. The KI of all analyzed samples varies approximately 0.136 to 0.458 Δ° 2Θ CuKα. Almost all obtained KI values are indicative of epimetamorphic conditions of approximately 300 – 350°C (KI < 0.250 Δ° 2Θ CuKα; Tab. 3), unless they result from the occurrence of detrital micas. Only two samples deviate from those, in case of sample BBB 11-09 anchi-metamorphic (< 2 µm) conditions and for sample BBB 13-09 diagenetic (< 0.2 µm) conditions can be identified. In spite of the small number of samples, a decreasing KI value from the interior basin to the margin can be observed, which corresponds to an increase in the stacking ordering and

Table 2. Semi-quantitative results of X-ray diffraction analyses

Sample	Qtz	Ill	Kln	Prl	Gbs	Kfs	Hem	Gth	Glt
BBB 11-09	-	+	++	-	-	-	-	-	-
BBB 13-09	++	+	++	0	0	-	-	-	-
BBB 29-09	++	+	++	-	-	0	0	-	-
BBB 32-09	++	++	+	-	-	-	-	0	-
BBB 33-09	++	++	+	-	-	-	-	0	-
BBB 34-09	++	++	+	0	-	-	0	-	-
BBB 38-09	++	++	+	-	0	0	0	-	0
CHD-R-C3	++	++	+	-	-	0	0	-	-
CHD-R-D3	-	++	-	-	-	-	-	-	-
CHD-R-D4	++	++	+	0	-	0	-	-	-

++ = principal component; + = abundantly present; 0 =appears in traces only; - = not identified; Qtz= quartz; Ill= illite; Kln= kaolinite; Prl= pyrophyllite; Gbs= gypsum; Kfs=k-feldspar; Hem= hematite; Gth= goethite; Glt= glauconite.

higher metamorphic conditions (Fig. 3). Hence, as the major part of the samples show epimetamorphic conditions, the age data should be interpreted as cooling ages during retrograde metamorphism. Any detrital memory in the investigated fine fractions was certainly removed. It can be noted that increasing metamorphic conditions (decreasing KI values) do not correlate with the stratigraphic position within the succession.

Polytype

The (060) and *hkl* XRD peaks of randomly oriented powder samples were used to distinguish different illite polytypes of the metapelitic samples either detrital $2M_1$ or different generations of authigenic $1M_d$ and 1M polytypes. The samples always reflect a mixture of the three polytypes with varying amounts depending on the grain size fractions. A general trend shows that the percentage of $2M_1$ illite decreases as particle size decreases. Correspondingly, the amount of $1M_d$ polytype decreases with increase in grain size. Most samples contain variable amounts of $1M_d$/1M and $2M_1$ illites (Tab. 3), whereas $2M_1$ illite is generally the main component even in the < 0.2 µm fraction. This is not the case for samples BBB 11-09 and BBB 13-09, which show $1M_d$/1M illite as dominant polytype in all three size fractions. The < 0.2 µm fraction is relatively enriched in most recently grown 1M illite, which crystallized in the final phase of metamorphism (Lee *et al.* 1989). Samples from the northern and southern Chapada Diamantina show a $2M_1$ proportion from 50 to 90%. As there was insufficient material for sample BBB 34-09 no data were acquired. Although the content of obtained polytypes correlates with the KI, and hence, with the intensity of deformation, there is no correlation between the KI values and the stratigraphic position of the samples

K/Ar age data

The 10 analyzed samples from metapelitic rocks (total 29 grain size fractions) provide age values ranging from 1,265.4 ± 18 Ma for BBB 11-09 (2 – 6 µm) to approximately 447.8 ± 6.9 Ma for BBB 33-09 (< 0.2 µm). The results are presented in Tab. 3 and Fig. 4. As there was relatively little material for BBB 11-09, no < 0.2 µm fraction could be separated. Radiogenic ^{40}Ar content ranges between 92.29 and 99.38%, indicating reliable analytical conditions for all analyses. The potassium content in the studied samples ranges from 1.61 to 9.11 K_2O%. This large scatter results from mixing with other fine-grained minerals in the fine mineral fractions. The measured age data change with particle size and polytype. Three age groups are found, depending on their location within the Espinhaço Basin and Chapada Diamantina: (1) The northern Chapada Diamantina yield ages in the < 2 µm fraction to be approximately 582.9 ± 8.7 to 644.9± 9.6 Ma for the CHD-R-C3, CHD-R-D3 and CHD-R-D4 samples. The recorded distribution of different grain size fractions in these samples overlaps within errors. (2) The central Chapada Diamantina yield ages between 1,090 ± 16 Ma (< 2 µm) and 1,265 ± 18 Ma (2 – 6 µm) for sample BBB 11-09 and 616±9.2 Ma (< 0.2 µm) to 731±10.9 Ma (2 – 6 µm) for sample BBB 13-09. The large age gap within the grain size fractions indicates a contamination with detrital micas. (3) The southern Chapada Diamantina yield ages in the range from 469 to 448 Ma (< 2 µm) for the most reliable samples (BBB 32-09, BBB 33-09, and BBB 34-09).

Table 3. Compilation of the K/Ar ages, illite crystallinity and illite polytypism of the investigated mineral fractions

Sample	Grain-size fraction	K/Ar Data					Illite crystallinity		Polytype		
		K_2O [wt%]	$^{40}Ar^*$ [nl/g] STP	$^{40}Ar^*$ [%]	Age [Ma]	±2σ-error [Ma]	air dry [Δ°2θ]	glycolated [Δ°2θ]	[%]		
									$2M_1$	1M	$1M_d$
BBB 11-09	< 2 µm	3.98	192.10	99.32	1089.8	16.3	0.267	0.283	29	9	62
	2 – 6 µm	1.61	95.23	98.89	1265.4	18.0	0.163	0.178	46	10	44
	< 0.2 µm	6.61	156.52	99.15	616.0	9.2	0.445	0.458	6	9	83
BBB 13-09	1 – 2 µm	4.20	112.60	97.00	684.1	6.3	0.232	0.239	17	15	69
	2 – 6 µm	4.58	133.04	99.24	730.6	10.9	0.189	0.198	45	14	41
	< 0.2 µm	2.17	44.69	97.25	546.7	8.2	0.138	0.148	34	7	60
BBB 29-09	< 2 µm	2.48	52.17	97.96	556.8	8.4	0.171	0.174	55	11	33
	2 – 6 µm	3.66	78.46	98.72	565.9	8.5	0.138	0.147	77	17	5
	< 0.2 µm	4.45	75.46	98.49	460.4	6.9	0.151	0.179	60	5	35
BBB 32-09	< 2 µm	7.53	130.41	99.21	470.1	7.0	0.154	0.164	68	6	26
	2 – 6 µm	8.52	148.68	99.26	473.2	7.1	0.134	0.139	94	< 5	< 5
	< 0.2 µm	4.41	72.30	92.29	447.8	6.9	0.160	0.163	48	4	47
BBB 33-09	< 2 µm	7.12	121.77	98.89	464.9	6.9	0.160	0.166	65	5	30
	2 – 6 µm	8.07	148.68	99.31	496.3	7.4	0.139	0.153	78	4	18
	< 0.2 µm	4.91	82.66	90.62	458.5	7.1	0.159	0.158	–	–	–
BBB 34-09	< 2 µm	5.33	92.09	93.56	469.1	7.2	0.129	0.144	–	–	–
	2 – 6 µm	7.59	136.48	97.23	485.9	7.3	0.142	0.147	–	–	–
	< 0.2 µm	8.28	150.46	98.07	490.3	7.4	0.178	0.185	58	10	32
BBB 38-09	< 2 µm	8.86	163.92	98.50	498.1	7.5	0.177	0.185	66	9	25
	2 – 6 µm	7.89	154.56	99.22	523.6	7.8	0.133	0.139	88	8	4
	< 0.2 µm	8.51	186.21	99.13	575.9	8.6	0.158	0.157	65	7	28
CHD-R-C3	< 2 µm	9.11	202.15	99.24	582.9	8.7	0.156	0.162	74	6	20
	2 – 6 µm	7.35	170.13	99.38	604.2	9.0	0.152	0.154	91	5	4
	< 0.2 µm	7.84	189.95	99.00	625.3	9.3	0.148	0.153	43	5	52
CHD-R-D3	< 2 µm	8.14	203.50	99.29	644.9	9.6	0.142	0.136	60	6	34
	2 – 6 µm	7.90	193.72	98.98	634.5	9.5	0.148	0.150	85	6	9
	< 0.2 µm	8.38	193.36	98.90	602.6	9.0	0.147	0.149	64	6	30
CHD-R-D4	< 2 µm	8.83	210.93	99.30	620.5	9.3	0.161	0.167	70	6	24
	2 – 6 µm	8.09	201.93	99.00	644.0	9.6	0.149	0.150	85	8	10

*Radiogenic.

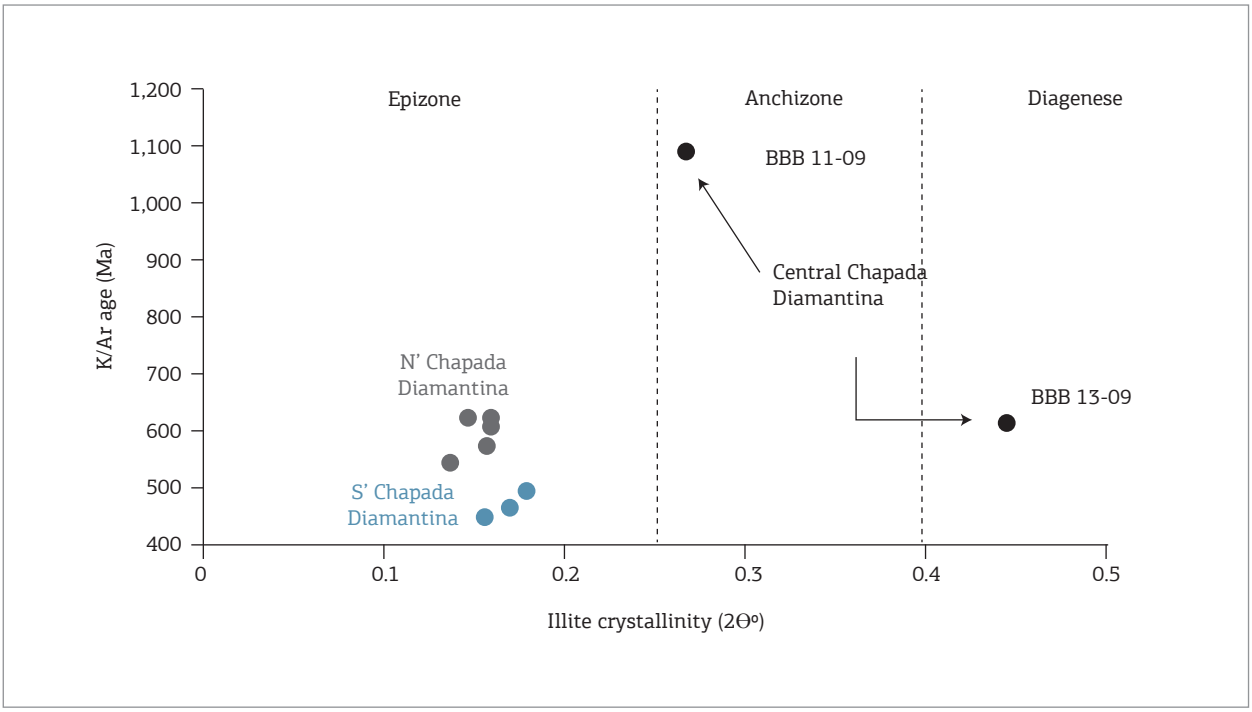

Figure 3. Regional relationship between Kübler Index (illite crystallinity) and K/Ar ages for the < 0.2 µm size fraction. A decreasing KI from the interior basin to the margin can be observed, which corresponds to an increase in the stacking order and higher metamorphic conditions.

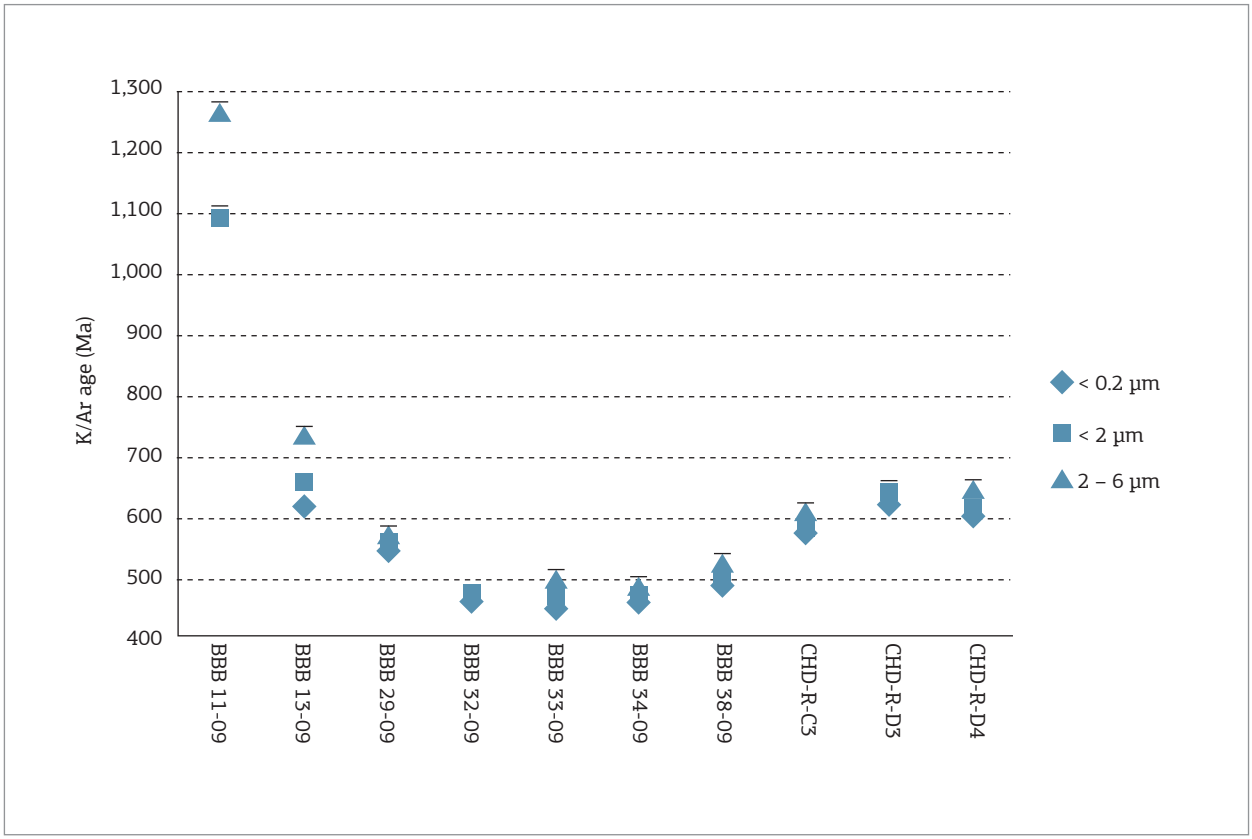

Figure 4. Results from K/Ar analyses in different grain size fractions (2σ, Error).

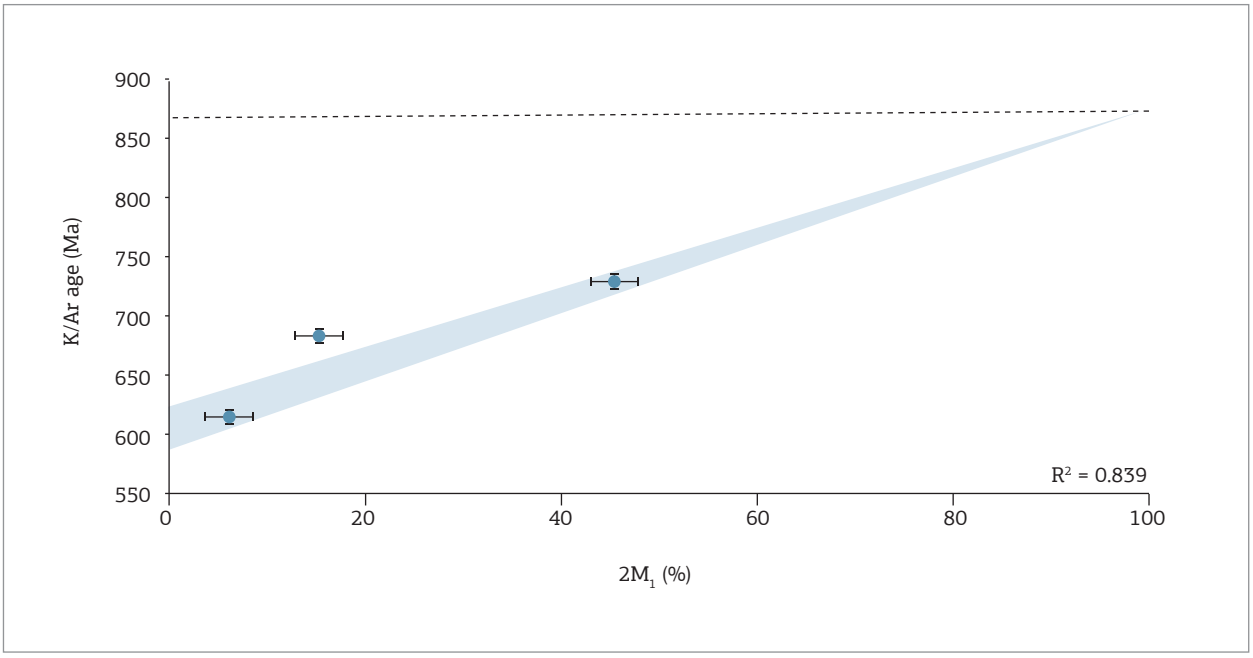

Figure 5. K/Ar ages with error bars (2σ) vs $2M_1$ (%) for the sample BBB 13-09, showing a diagenetic age of 616 – 600 Ma and an age of 870 Ma for the last thermal event (> 300°C).

DISCUSSION

The following section reviews the most important approaches to interpret fine-fraction data:

The crucial aspect, however, is the temperature, which reaches at the maximum of the metamorphism. On the one hand, it controls the neocrystallization of illite and its crystallinity, on the other hand, exceeding closing temperature leads to a resetting of the mineral ages. The understanding of the closing behavior of small illite crystals has a fundamental influence on the interpretation. The importance of the effective diffusion radius on the closure temperature for the Ar system has been shown by a large number of reports (e.g. Dahl 1996; Villa 1998; Hodges 2003). These studies focused on white micas with grain sizes > 200 µm. Hunziker *et al.* (1986) indicated a closure temperature interval of 260 ± 30°C for the mica fractions < 2 µm, whereas Wemmer and Ahrendt (1997) reported K/Ar ages on fine-grained white mica (sericite < 2 µm) that did not behave as open systems, confirming that even temperatures approximately 275°C did not reset the Ar-system. Therefore, the closure temperature of fine-grained mica has to be estimated somewhere between 275 and 350°C for grain size fractions < 2 µm (Wemmer & Ahrendt 1997). However, this value is significantly lower than the closure temperature interval 350 ± 50°C for coarse-grained micas recommended by Purdy and Jäger (1976) and McDougall and Harrison (1999). Attention should also be given to the case of a potential contamination by other K-bearing phases. Potassium feldspar, for example, can make the age appear younger due to the lower closing temperature (Fitz-Gerald & Harrison 1993). Otherwise, Zwingmann *et al.* (2010) showed that K/Ar ages of fault gouge samples from the Swiss Alps are independent of K-feldspar content. This suggests that the fine-grained feldspar contaminant was isotopically reset during deformation approximately at the same time when illite growth occurred. Focus should be given on the problem that might result due to a mixture of different generations of illite growth. In general, the smallest grain size fractions (< 0.2 µm) are the least contaminated, and therefore, closest to the age of the youngest deformation event and should represent the most recently grown illites. Similar increases in both the K/Ar age data and the $2M_1$ content with increasing grain size, representing earlier illite-forming events, have been reported in many previous studies (e.g. Hower *et al.* 1963; Grathoff & Moore 1996; Clauer *et al.* 1997; Grathoff *et al.* 1998). A highly simplified scheme to interpret K/Ar ages in various scenarios of mixing different polytypes is given in Marheine (1997). In principal, in low-grade sedimentary rocks, it can be assumed that the $2M_1$ polytype is detrital whereas the 1M and $1M_d$ polytype are authigenic products formed during diagenesis to anchi-metamorphic conditions during subsequent burial (e.g. Grathoff & Moore 1996). On the basis of XRD, the $2M_1$ illite cannot be distinguished from detrital micas (also a $2M_1$ polytype). Only the combined application of these independent results (age data, KI values and polytype proportions) allows differentiating between both. Type $2M_1$ illite forms at temperatures approximately 200 – 250°C (Velde 1965), and if the diagenetic reaction from $1M_d$ to 1M and

finally to $2M_1$ from laboratory experiments of Velde (1965) also applies for metapelitic rocks, high concentration of $2M_1$ illite can be used as an additional indicator for temperature (>>200°). $1M/1M_d$ are thought to form at significantly lower temperatures, below 200°C (Velde 1965). $2M_1$ illite should be expected in shales because its source is the weathering mica flakes of the host rock.

The results of K/Ar geochronology (Tab. 3) of metapelitic rocks show that three domains can be distinguished: northern, central and southern Chapada Diamantina. These domains differ in their age and structural configuration. The latest Brasiliano overprint was indentified in the southern Chapada Diamantina, the oldest deformation age in the northern Chapada Diamantina.

The northern Chapada Diamantina comprises the SW-NE-trending Mesoproterozoic sediments of the Espinhaço Supergroup northeast of the Irecê basin. The investigated samples of this area (CHD-R-D3 and CHD-R-D4) yield an average age of 632.7 ± 9.5 Ma in the < 2 µm fraction, indicating a maximum age for the latest deformation and peak metamorphism. The final growth of illites is dated at 614 ± 9.1 Ma (< 0.2 µm fraction). As all samples yield KI values characteristic for epimetamorphic conditions, it is to be expected that all authigenic prograde-formed illites completely transformed from $1M_d/1M$ to $2M_1$. Still more evidence for the onset of deformation under epizonal conditions is supported by the high amount of $2M_1$ illites, which even in the smallest grain size fraction (< 0.2 µm) exceeds 60%. Therefore, the occurrence of 1M and $1M_d$ illite can be explained by retrograde metamorphism and growth during decreasing temperatures. Hence, the data can at best be described as cooling ages, which implies that the < 2 µm fraction should be closer to the peak metamorphism than the < 0.2 µm fraction. As the $1M/1M_d$ content is relatively low, it is indicative of a rapid single-phase cooling history. Thus, it is clear that the age of the authigenic illite is also the age of the last deformation event. However, it remains questionable whether the slightly younger age of the sample CHD-R-C3 of 582.9 ± 8.7 Ma (< 2 µm fraction) can be attributed to local tectonic activities or an alteration/regional fluid migration effect. However, rejuvenation due to potassium-bearing mineral phase can be excluded from the XRD data.

The K/Ar fine-fraction ages are synchronous with a widespread Precambrian deformation event located between the northern margin of the São Francisco Craton and the Pernambuco-Alagoas massif (approximately 200 – 250 km to the north of CHD-R-D4) that culminated in the final assembly of West Gondwana. This event resulted among other structural elements in SW-trending fold axes and built up the Riacho do Pontal belt. Brito Neves *et al*. (1980, 1999) described that age data approximately 630 Ma, which have been inferred for the main phase of folding, whereas post-tectonic plutons are dated between 580 and 540 Ma (Rb-Sr; Jardim de Sá 1994). Within the northern Chapada Diamantina, the deformation and thermal stress were completed at that point, while apparently at least 100 km to the north in the Riacho do Pontal belt the collision continued. The supposed age of 630 Ma for the major peak of metamorphism could be confirmed with unpublished U-Pb and Rb-Sr data (Brito Neves, in preparation) and is identical to our data as well as the structural alignment of SW-trending fold axes in the northern Chapada Diamantina.

The results derived from illite polytype quantification and age dating indicate that post-tectonic plutonism, which occurred in the Borborema province, did not affect the Mesoproterozoic Espinhaço Supergroup of the northern Chapada Diamantina. This appears also to be in good agreement with the observation of a northward increasing of deformation made by Inda and Barbosa (1978).

A resetting of the isotopic and magnetic systems that affected the Neoproterozoic sediments of the Irecê basin and the mesoproterozoic Caboclo formation at approximately 520 Ma can be attributed to a regional-scale fluid migration and mineralization as a repercussion of the Brasiliano orogenic cycle (Cunha *et al*. 2003; Trindade *et al*. 2004; Texeira *et al*. 2010) and is, therefore, negligible in this context.

The central Chapada Diamantina is bounded by the Irecê basin to the west and the Jacobina belt to the east. The samples BBB 11-09 and BBB 13-09 can be assigned to this region. BBB 11-09 of the Caboclo formation yield ages of 1,089.8 ± 16.3 (< 2 µm fraction) and 1,265.4 ± 18 Ma (2 – 6 µm fraction). The interpretation of this data is affected by the lack of the < 0.2 µm fraction, which is most sensitive for thermal impulses. Owing to the large age difference within the two size fractions, it can be assumed that these ages do not correspond to the total resetting of the isotopic clock. Therefore, these are meaningless mixed ages of detrital and authigenic minerals. This is supported by the KI values indicative of anchizonal metamorphic conditions and the low content of $2M_1$ illite, giving evidence for, if at all, weak deformation intensity. The high $1M/1M_d$ content of 60% is probably due to a weak retrograde overprint/alteration involving new growth of low-temperature clay minerals. Thus, two conclusions can be drawn: first, the deformation was insufficient to reset the detrital age of the illites, and second, the results cannot be assigned to a Brasiliano deformation event as it was identified in the northern and southern Chapada Diamantina. This seems plausible because the sediments of the Morro do Chapéu and Ventura area are covering the archaic rocks of the Gavião/Lençois block, which is considered to be geologically stable.

BBB 13-09 was investigated in more detail and shows a relatively large time period from 616 ± 9.2 Ma in the smallest size fraction to 730.6 ± 10.9 Ma in the 2 – 6 µm size fraction. The age of the < 0.2 µm fraction corresponds to the deformation of the northern Chapada Diamantina, indicating that at least the smallest size fraction adapt to the last low-grade thermal event. The decrease in temperature is followed by a decrease in deformation intensity as can be observed by KI and illite polytypism. The apparent diagenetic and detrital ages of the illites using linear extrapolation, read from Fig. 5, are 616 – 610 and 870 Ma. We say apparent because these are calculated ages for the two extreme cases: 100% $1M/1M_d$ and 100% $2M_1$. The upper limitation for the apparent diagenetic age is given by the < 0.2 µm age because even the smallest size fraction is not completely free from $2M_1$ illite. The extrapolated "detrital" component age for BBB 13-09 yielded an age of approximately 860 Ma. As this age is significantly less than the stratigraphic age (> 1,200 Ma); it clearly does not reflect the real sedimentary detritus. It is apparent that the coarser size fractions contain varying components of two illite polytype populations, an older $2M_1$ polytype (probably detrital muscovite that gives an averaging age of the formation of the $2M_1$ polytype in their pre-depositional provenance areas) and a younger synkinematic 1M illite. However, the detrital component reflects a total reset that is not related to the visible deformation but presumably related to a thermal event (> 350°C). This event can be related to an episode of rifting that affected the interior of the São Francisco Craton and began probably approximately 900 Ma (Pedrosa-Soares *et al*. 2001; Tack *et al*. 2001).

Taking all the results into account, it is likely that the sediments in this region were less strongly affected by the collision at the northern craton margin than the samples belonging to the northern Chapada Diamantina discussed above, and in addition, there are no indications of intra-plate tectonic episodes of "Grenvillian-type age" that triggered new growth of illite.

The southern Chapada Diamantina comprises the area situated to the south of the Irecê basin with mainly NNW-SSE-trending fold axes from where samples BBB 29-09, BBB 32-09, BBB 33-09, BBB 34-09 and BBB 38-09 were obtained. Samples BBB 32-09, BBB 33-09 and BBB 34-09 are of particular interest as they were taken directly from the hinge zone. Hinge zones are characterized by a pronounced cleavage in which new growth of synkinematic minerals is expected and, therefore, the deformation is highly preserved. The last illite growth, and therefore the last deformation of the southern Espinhaço Supergroup, occurred between 460.4 ± 6.9 and 447.8 ± 6.9 Ma (< 0.2 µm fraction). The < 2 µm fraction recorded slightly older ages in the range of 470.1 ± 7 to 464.9 ± 6.9 Ma. These samples show overlapping ages within errors, suggesting the absence of detrital contamination and a synchronous deformation history independent of the stratigraphic position (Ouricuri do Ouro Fm – Guiné Fm.). As the KI data yield epizonal conditions, it can be assumed that the fine fractions are composed of recessed detrital micas and retrograde-formed authigenic illites. The shown polytype data, high $2M_1$ and low $1M/1M_d$ content, in combination with the age data suggest a short-lived deformation event approximately 470 Ma and a single-phase rapid-cooling path. The slightly younger age of the sample BBB 33-09 is reflected in the lower $2M_1$ content, probably caused by a local alteration effect. Thus, more emphasis should be given to the ages of samples BBB 32-09 and BBB 34-09 as maximum ages for the final metamorphism. The slightly older ages of samples BBB 38-09 and BBB 29-09 are a combination of the regional distribution and structural position. Both samples were not taken from hinge zones and are therefore less deformed.

The large synclines and anticlines at the eastern margin of the Paramirim impactogen, extending along hundreds of kilometers with NNW-SSE trends, are related to the formation of the Araçuaí belt, which is now identified as a late stage Brasiliano event approximately 470 Ma. In addition, this interpretation is supported by both Danderfer and Dardenne (2002) and Cruz and Alkmim (2006) who postulated that the Paramirim impactogen underwent partial inversion during the Brasiliano orogeny. In the southern two thirds of the impactogen, this inversion reactivated pre-existing normal faults and transfer faults to generate NNW-trending basement-involved thrust faults linked by strike slip shear zones (Alkmim *et al*. 2006). As the NNW-trending faults and folds of the Paramirim impactogen, which formed during the inversion, overprint the E-W-trending thrust and folds of the Rio Padro Salient, they are probably younger (Cruz & Alkmim 2006). This seems to be reasonable regarding the latest post-collisional activity approximately 490 Ma within the Araçuaí orogeny (Pedrosa-Soares *et al*. 2008).

By comparison, the age data obtained in this study are slightly younger than K/Ar hornblende cooling ages of the São Timoteo Granite in the Lagoa Real complex (ca. 100 km in the southwest of localities of samples BBB 32-09, BBB 33-09 and BBB 34-09) dated at 510 – 490 Ma by Cordani *et al*. (1992). Turpin *et al*. (1988) interpreted discordant zircon U/Pb ages approximately 500 Ma as the age of metamorphism of the Lagoa Real complex. This coincides with that reported by Pimentel *et al*. (unpublished data) on zircon and sphene grains of the same complex that yielded discordant ages with an upper intercept at 1,740 Ma and a lower intercept at 490 Ma. The slightly lower fine-fraction ages (approximately 30 Ma), found in this study, can be

explained due to the higher stratigraphic position and the lower closing temperature. Therefore, they are attributable to the thermal event that also affected the Lagoa Real complex and provide evidence for a wide-ranging deformation event. On the basis of the K/Ar fine-fraction data, a reactivation and inversion of the Paramirim impactogen and folding after 460 Ma can be excluded.

CONCLUSION

The K/Ar ages presented here suggest that the portion of the Espinhaço Supergroup, which crops out in the Chapada Diamantina, underwent metamorphism and deformation in various areas at different times, leading to the formation of distinct structural features. The deformation of the northern Chapada Diamantina occurred in the course of the collision between the northern margin of the São Francisco Craton and the Pernambuco-Alagoas massif. This event resulted in SW-trending fold axes and built up the Riacho do Pontal belt. K-Ar fine-fraction dating yield an age of 630 Ma for this event, which is coeval to the peak metamorphism in the Riacho do Pontal belt. Till now, no statement can be made on the N-S/NNW-SSE-trending axes of the sediments in the area east of the Irecê basin. The deformation of the southern Chapada Diamantina was established in conjunction with the emergence of the Araçuai orogen and the inversion and reactivation of the Paramirim impactogen. The final deformation phase is recorded by the K/Ar fine-fraction dating in the range between 470 and 460 Ma.

REFERENCES

Ahrendt H., Hunziker J., Weber K. 1978. K/Ar-Altersbestimmungen an schwach metamorphen Gesteinen des Rheinischen Schiefergebirges. *Zeitschrift der Deutschen Geologischen Gesellschaft Band*, **129**:229-247.

Alkmim F.F., Marshak S., Pedrosa-Soares A.C., Peres G.G., Cruz S.C.P., Whittington A. 2006. Kinematic evolution of the Araçuaí-West Congo orogen in Brazil and Africa: nutcracker tectonics during the Neoproterozoic assembly of Gondwana. *Precambrian Research*, **149**:43-64.

Alvarenga F.F., Dardenne M.A. 1978. Geologia dos Grupos Bambui e Paranoá na Serra de São Domingos, Minas Gerais XXX. *In:* SBG, Congresso Brasilieiro de Geologia, Recife, Anais, vol. 2, p. 546-556.

Babinski M. 1993. *Idades isocrônicas Pb/Pb e geoquímica isotópica de Pb nas rochas carbonáticas do Grupo Bambuí na porção sul da bacia do São Francisco*. Unpublished PhD Thesis, Universidade de São Paulo, SP, 133 p.

Brito Neves B.B.,Cordani U.G., Torquato J.R. 1980. Evolução geocronológica do Estado da Bahia. *In:* Inda H., Duarte A.V (eds.). *Geologia e recursos minerais do estado da Bahia: textos básicos*. Salvador, CPM/SME, vol. 3, p. 1-101.

Brito Neves B.B., Campos Neto M.C., Fuck R.A. 1999. From Rodinia to Western Gondwana: an approach to the Brasiliano-Pan African Cycle and orogenic collage. *Episodes*, **22**:155-166.

Brito Neves B.B., Dos Santos R.A., Cruz Campanha G.A. 2012. A discordância angular e erosive entre os grupos Chapada Diamantina e Bambuí (Una) na folha Mirangaba-Bahia. *Geologia USP, Série Científica*, **12**:99-114.

Clauer N., Rais N., Schaltegger U., Piqué A. 1995. K-Ar systematics of clay-to-mica minerals in a multi-stage low-grade metamorphic solution. *Chemical Geology*, 124:305-316.

Clauer N., Srodon J., Francu J., Sucha V. 1997. K-Ar dating of illite fundamental particles separated from illite-smectite. *Clay Minerals*, **32**:181-196.

Cordani U.G., Iyer S.S., Taylor P., Kawashita K., Sato K., McReath I. 1992. Pb–Pb, Rb–Sr and K–Ar systematic of the Lagoa Real uranium province (south-central Bahia, Brazil) and the Espinhaço cycle. *Journal of South American Earth Sciences*, **5**:33-46.

Cordani U.G., Fraga L.M., Reis N., Tassinari C.C.G., Neves B.B. 2010. On the origin and tectonic significance of the intra-plate events of Grenvillian-type age in South America: a discussion. *Journal of South American Earth Sciences*, **29**:143-159.

Cruz S.C.P., Alkmim F.F. 2006. The tectonic interaction between the Paramirim Aulacogen and the Araçuai belt, São Francisco Craton Region, Eastern Brazil. *Anais da Academia Brasileira de Ciências*, **78**:151-173.

Cunha I.A., Vasconcelos P., Babinski M., Misi A., Franca-Rocha W.J.S. 2003. $^{40}Ar/^{39}Ar$ muscovite ages from hydrothermal altered dolostone hosting the Pb-Ag Caboclo deposit, Bahia, Brazil. *In*: SSAGI, South American Symposium on Isotope Geology, *Short Papers*, IV.

Dahl P. S. 1996. The crystal–chemical basis for Ar retention in micas: inferences from interlayer partitioning and implications for geochronology. *Contributions to Mineralogy and Petrology*, **123**:22-39.

Danderfer A. 2000. *Geologia Sedimentar e Evolucão Tectônica do Espinhaço Setentrional*. Doctor Thesis, Universidade de Brasília, Brazil, 498 p.

Danderfer F. A., Dardenne M.A. 2002. Tectonoestratigrafia da bacia Espinhaço na porção centronorte do Cráton do São Francisco: registro de uma evolução poliistórica descontínua. *Revista Brasileira de Geociências*, **4**:449-460.

Danderfer F. A., De Waele B., Pedreira A. J., Nalini H. A. 2009. New geochronological constraints on the geological evolution of Espinhaço basin within the São Francisco Craton—Brazil. Precambrian Research **170**: S. 116-128.

Fitz-Gerald J., Harrison T. 1993. Argon diffusion domains in K-feldspar; I, Microstructures in MH10. *Contributions to Mineralogy and Petrology*, **113**:367-380.

Fuck R.A., Brito Neves B.B., Schobbenhaus C. 2008. Rodinia descendants in South America. *Precambrian Research*, **160**:108-126.

Fuhrmann U., Lippolt H.J., Hess J.C. 1987. Examination of some proposed K–Ar standards: 40Ar/39Ar analyses and conventional K–Ar data. *Chemical Geology (Isotope Geoscience Section)*, **66**:41-51.

Grathoff G.H., Moore D.M. 1996. Illite polytype quantification using WILDFIRE calculated X ray diffraction patterns. *Clays and Clay Minerals*, **44**:835-842.

Grathoff G., Moore D., Hay R., Wemmer K. 1998. Illite polytype quantification and K/Ar dating of paleozoic shales: a techniquento quantify diagenetic and detrital illite. *In*: Schieber J., Zimmerle W., Sethi P. (eds.). *Shales and Mudstones II*. Schweizerbart, Stuttgart, p. 161-175.

Hodges K. V. 2003. Geochronology and thermochronology in orogenic systems. *In*: Rudnick R.L. (ed.). *Treatise on Geochemistry: The Crust*, Elsevier Science, Amsterdam, vol. 3, p. 263-292.

Hower J., Hurley P.M., Pinson W.H., Fairburn H.W. 1963. The dependence of K-Ar age on the mineralogy of various particle size ranges in a shale. *Geochimica et Cosmochimica Acta*, **27**:405-410.

Hunziker J.C., Frey M., Clauer N., Dallmeyer R.D., Friedrichsen H., Flehmig W., Hochstrasser K., Roggwiler P., Schwander H. 1986. The evolution of illite to muscovite: mineralogical and isotopic data from the Glarus Alps, Switzerland. *Contributions to Mineralogy and Petrology*, **92**:157-180.

Inda H.A.V., Barbosa J.F. 1978. Nota Explicativa para o Mapa Geol¢gico do Estado da Bahia – escala 1:1.000.000. Salvador, SME/CPM, p. 137.

Jardim de Sá E.F. 1994. *A Faixa Seridó (Província Borborema, NE do Brasil) e o Seu Significado Geodinâmico na Cadeia Brasiliana/Pan-Africana*. Tese de Doutorado, Universidade de Brasília, Brasıília DF, Brazil, p. 795.

Kübler B. 1967. La cristallinité de l'illite et les zones tout á fait supérieurs de métamorphisme. Colloque sur les "Etages Tectoniques", 18-21. avrile 1966, Festschrift: p. 105-122, Neuchâtel.

Lee M., Aronson J. L., Savin S.M. 1989. Timing and conditions of Permian Rotliegende Sandstone Diagenesis, Southern North Sea: K/Ar and oxygen isotopic data. *American Association of Petroleum Geologists Bulletin*, **73**:195-215.

Machado N., Schrank A., Abreu F.R., Knauer L.G., Abreu P.A.A. 1989. Resultados preliminares da geocronologia U–Pb na Serra do Espinhaço Meridional. *Proceedings of the 58 Simpó sio de Geologia de Minas Gerais. Sociedade Brasileira de Geologia SBG-MG*, Belo Horizonte, Anais, p. 171-174.

Marheine D. 1997. Zeitmarken im variszischen Kollisionsberreich des Rhenoherzynikums-Saxothuringikums zwischen Harzund sächsischem Granulitmassiv–Ergebnisse von K/Ar-Altersbestimmungen. *Göttinger Arbeiten zur Geologie und Paläontologie*, **75**:1-97.

McDougall I., Harrison T.M. 1999. *Geochronology and Thermochronology by the $^{40}Ar/^{39}Ar$ Method*, 2nd ed. New York, Oxford: Oxford University Press.

Misi A., Veizer J. 1998. Neoproterozoic carbonate sequences of the Una Group, Irecê Basin, Brazil: chemostratigraphy, age and correlations. *Precambrian Research*, **89**:87-100.

Moore D.M., Reynolds R.C. Jr. 1997. *X-Ray Diffraction and the Identification and Analysis of Clay Minerals*, 2nd ed. , Oxford, New York: Oxford University Press.

Pedreira A. J. 1994. O Supergrupo Espinhaço na Chapada Diamantina Centro-oriental, Bahia: Sedimentologia, Estratigrafia e Tectônica. PhD Thesis, Instituto de Geociências, Universidade de São Paulo.

Pedreira A.J., De Waele B. 2008. Contemporaneous evolution of the Palaeoproterozoic-Mesoproterozoic sedimentary basins of the São Francisco-Congo Craton. *Geological Society, London, Special Publications*, **294**(1):33-48.

Pedreira A. J., Rocha, A. J. D. 2004. Revisa˜o estratigra ´fica do Grupo Chapada Diamantina, Bahia. In: Congresso Brasileiro de Geologia 42, Araxá, Anais. Sociedade Brasileira de Geologia. (CD-ROM).

Pedrosa-Soares A., Alkmim F. F., Tack L., Noce C. M., Babinski M., Silva L. C., Martins Neto ,M.A. 2008. Similarities and differences between the brazilian and african counterparts of the neoproterozoic aracuai-west congo orogen.Geological Society Special Publications, 294, 153-172. doi: http://dx.doi.org/10.1144/SP294.9

Pedrosa-Soares A.C., Noce C.M., Wiedemann C.M., Pinto C.P. 2001. The Araçuai-West Congo orogen in Brazil: an overview of aconfined orogen formed during Gondwanaland assembly. *Precambrian Research*, **110**:307-323.

Pevear D.R. 1992. Illite age analysis, a new tool for basin thermal history analysis. *In*: Kharaka Y.K. and Maest A.S. (eds.). *Proceedings of the 7th International Symposium on Water-Rock Interaction (offprint)*, Park City, UT, Water-Rock Interaction, p. 1251-1254.

Purdy J.W., Jäger E. 1976. K/Ar ages of rock-forming minerals from the Central Alps. *Memoirs of the Institute of Geology and Mineralogy, University of Padova*, **30**:1-31.

Schobbenhaus C. 1996. As tafrogêneses superpostas Espinhaço e Santo Onofre, Estado da Bahia: revisão e novas propostas. *Revista Brasileira de Geociências*, **26**(4):265-276.

Schuhmacher E. 1975. Herstellung von 99.9997% ^{38}Ar für die $^{40}K/^{40}Ar$ Geochronologie. *Geochron. Chimia*, **24**:441-442.

Steiger, R. H., Jäger, E. 1977. Subcommision on geochronology; convention on the use of decay constants in geo- and cosmochronology. *Earth Planetary Science Letters*, **36**:358-362.

Tack L., Wingate M.T.D., Liégeois J.-P., Fernandez-Alonso M., Deblond A. 2001. Early Neoproterozoic magmatism (1000–910 Ma) of the Zadinian and Mayumbian Groups (Bas-Congo): onset of Rodinian rifting at the western edge of the Congo craton. *Precambrian Research*, **110**:277-306.

Texeira J.B.G., Da Glória da Silva M., Misi A., Pereira Cruz S.C., Da Silva Sá J.H. 2010. Geotectonic setting and metallogeny of the northern São Francisco craton, Bahia, Brazil. *Journal of South American Earth Sciences*, **30**:71-83.

Torquato J.R., Fogaça A.C.C. 1981. Correlações entre o Supergrupo Espinhaço no Brasil, o Grupo Chela em Angola e as formações Nosib e Khoabendus da Namíbia. *In*: *Simpósio Crató do Sã o Francisco e suas faixas marginais*. Salvador, BA, Brasil, p. 87-98.

Trindade R.I.F., D'Agrella-Filho M., Babinski M., Brito Neves B.B. 2004. Paleomagnetism and geochronology of the Bebedouro cap carbonate: evidence for continental-scale Cambrian remagnetization in the São Francisco Craton, Brazil. *Precambrian Research*, **128**(2004):83-103.

Turpin L., Maruèjol P., Cuney M. 1988. U-Pb, Rb-Sr and Sm-Nd chronology of granitic basement, hydrotermal albitites and uranium mineralization, Lagoa Real, South Bahia, Brazil. *Contributions to Mineralogy and Petrology*, **98**:139-147.

Velde B. 1965. Phengite micas: synthesis, stability and natural occurrence. *American Journal of Science*, **263**:886-913.

Villa I.M. 1998. Isotopic closure. *Terra Nova*, **10**:42-47.

Weber K. 1972 Notes on determination of Illite crystallinity. *Neues Jahrbuch für Geologie und Mineralogie Monatshefte*, **1972**:267.

Wemmer K. 1991. K/Ar-Altersdatierungsmöglichkeiten für retrograde Deformationsprozesse im spröden und duktilen Bereich – Beispiele aus der KTB-Vorbohrung (Oberpfalz) und im Bereich der Insubrischen Linie (N-Italien). *Göttinger Arbeiten Geologie und Paläontologie*, **51**:61.

Wemmer K., Ahrendt H. 1997. Comparative K-Ar and Rb/Sr age determination of retrograde processes on rocks from the KTB deep drilling project. *Geologische Rundschau*, **86**:272-285.

Zwingmann H., Mancktelow N., Antognini M., Lucchini R. 2010. Dating of shallow faults: New constraints from the AlpTransit tunnel site (Switzerland). *Geology*, **38**:487-490.

Arquivo digital disponível on-line no site www.sbgeo.org.br